# 3s-proton occupancies in $^{204}$Hg and $^{206}$Pb

P. Grabmayr, A. Mondry, G. J. Wagner, and P. Woldt*
*Physikalisches Institut der Universität Tübingen, D-72076 Tübingen, Germany*

G. P. A. Berg, J. Lisantti, D. W. Miller, H. Nann, and E. J. Stephenson
*Indiana University Cyclotron Facility, Bloomington, Indiana 47405*
(Received 13 January 1994)

In parallel experiments angular distributions of the differential cross sections and vector analyzing powers have been measured for the $(\vec{d},^3\mathrm{He})$ reactions on $^{204}$Hg and $^{206}$Pb at an incident deuteron energy of 79.1 MeV. The $Q$ values for the reaction on $^{204}$Hg and a $^{202}$Hg contaminant were determined as $-3340.9(3.4)$ keV and $-2738.8(3.5)$ keV, respectively. Spectroscopic factors on $^{204}$Hg and $^{206}$Pb were obtained through a consistent distorted wave Born approximation (DWBA) analysis. A combined evaluation of relative spectroscopic factors and electron scattering (CERES) yields 3s-proton occupancies in $^{204}$Hg and $^{206}$Pb. The latter is compatible with an earlier CERES result based on the more accurately known $^{206}$Pb – $^{205}$Tl charge density difference. Substantial deviations from shell-model occupancies are observed.

PACS number(s): 25.45.Hi, 21.10.Jx, 21.10.Dr, 27.80.+w

## I. INTRODUCTION

The determination of the number of protons in a given shell-model orbital is of considerable interest for nuclear many-body theories. In principle it may be obtained from the infinite sum of spectroscopic factors [1] as derived from proton removal experiments such as $(d,^3\mathrm{He})$ or $(e,e'p)$ reactions. In practice, however, this method suffers from the model uncertainties of absolute spectroscopic factors and the impossibility of summing up to infinite separation energies. As a remedy a combined evaluation of relative spectroscopic factors and electron scattering (CERES) was proposed [2]. This method relies on the much more accurate relative spectroscopic factors and truncated sums over $\approx 1\hbar\omega$ in excitation energy. In addition, it employs the charge density differences as determined from elastic electron scattering on neighboring nuclei.

The applications of the CERES method to 3s-proton occupancies in nuclei in the Pb region have recently been reviewed [3]. Interestingly, they are exclusively based on the carefully measured difference of charge densities in $^{206}$Pb and $^{205}$Tl and its interpretation in the mean field [4, 5]. Together with a network of relative spectroscopic factors from proton removal experiments, 3s-proton occupancies of $(84 \pm 13)\%$ and $(74 \pm 11)\%$ were obtained [3] for $^{208}$Pb and $^{206}$Pb, respectively. These occupancies are higher, albeit compatible (within the combined errors), with those estimated from spectroscopic factors for $(e,e'p)$ [6–8] or $(d,^3\mathrm{He})$ [9] reactions or from the charge density difference alone [5].

In this situation a CERES analysis based on another pair of charge densities was certainly of interest. Such a pair became available when electron scattering on $^{204}$Hg was measured and the mean-field interpretation of the $^{206}$Pb–$^{204}$Hg charge density difference was given [10]. The contribution of 3s-protons to this difference was obtained as $z' = 1.02(10)$, in other words, the difference in the number of 3s-protons between $^{206}$Pb and $^{204}$Hg is about 1. This value represents an average of results from Hartree-Fock calculations with different forces. (We disregard the value resulting from use of the Tondeur force [11] which was designed to reproduce density distributions and does not claim predictive power for other properties.) The error encompasses the values from the three remaining forces.

With $z'$ available, the CERES method yields the following relation for the number of 3s protons in $^{206}$Pb:

$$n(206) \simeq z' \left[1 - \frac{\Sigma' S(204)}{\Sigma' S(206)}\right]^{-1} . \quad (1)$$

Here, $\Sigma' S(A)$ represents the summed spectroscopic factors $C^2S$ for 3s-proton removal from $^{204}$Hg and $^{206}$Pb, respectively. The $\Sigma'$ indicates a truncated sum over $\approx 1\hbar\omega$ excitation energy in the final nuclei $^{203}$Au and $^{205}$Tl, respectively. In a simple shell-model situation one expects $z' = 2$ due to an empty $3s_{1/2}$ shell in $^{204}$Hg, hence vanishing $n(204) = \Sigma S(204) \geq \Sigma' S(204)$. The quoted value of $z' \approx 1$ shows a considerable deviation from the simple shell-model picture.

The only existing information for spectroscopic strength on $^{204}$Hg stems from a $^{204}\mathrm{Hg}(\vec{t},\alpha)^{203}$Au experiment at 17 MeV [12]. In fact, this reaction was the major source of information on levels in $^{203}$Au [13], including its mass. This experiment also reveals the presence of substantial $3s_{1/2}$ strength in the ground state of $^{204}$Hg,

*Present address: Siemens, Erlangen, Germany.

 

indicative of deviations from the simple shell-model picture. However, due to the large momentum mismatch typical of $(t,\alpha)$ reactions the distorted wave Born approximation (DWBA) fits to the data were not very satisfactory and the spectroscopic factors are hardly reliable. This prompted our present study of the $^{204}$Hg($\vec{d}$,$^3$He) reaction at 80 MeV. As known from previous studies on neighboring nuclei, e.g. Refs. [9, 14], ($d$,$^3$He) reaction cross sections at this energy are well reproduced by DWBA calculations.

The CERES method also requires pickup data on $^{206}$Pb, as indicated in Eq. (1). Now, the $^{206}$Pb($d$,$^3$He) reaction has been measured at 52 MeV [15] and at 79.4 MeV [9]. The $s_{1/2}$ hole strength has also been studied in a high resolution $(e,e'p)$ experiment [16]. Nevertheless, we measured the $^{206}$Pb($\vec{d}$,$^3$He) reaction again as part of the present experiment. This was done by interchanging $^{204}$Hg and $^{206}$Pb targets frequently to minimize the experimental errors that might affect the ratio of spectroscopic factors entering Eq. (1). This procedure was expecially appropriate as the present experiment was the first ($d$,$^3$He) experiment with the new K600 spectrograph at the Indiana University Cyclotron Facility (IUCF). Hence it was important that all uncertainties of the K600 acceptances cancel out in the CERES application.

## II. EXPERIMENTAL PROCEDURE

The ($\vec{d}$,$^3$He) reactions on $^{204}$Hg and $^{206}$Pb were studied using a 79.1 MeV beam of vector-polarized deuterons at IUCF. Angular distribution measurements of the differential cross sections $d\sigma(\Theta)/d\Omega$ and vector-analyzing powers $iT_{11}(\Theta)$ were made. The outgoing $^3$He particles were detected with the K600 magnetic spectrograph at nominal laboratory angles of 6°, 9°, 12°, 15°, 17°, and 20°.

A $2'' \times 1''$ aperture at the spectrograph entrance defined the solid angle of about 2.5 msr with an angular opening of 4° in the scattering plane. The spectrograph was run in a dispersion-matching mode. Its focal plane was equipped with two vertical drift chambers and a plastic scintillation detector. Particle identification was achieved using a combination of time-of-flight and pulse-height information from the plastic scintillator. Position and angle of $^3$He particles striking the focal plane were measured by the drift chambers and recorded on event tape for off line analysis. Kinematical corrections and determination of the actual scattering angles were performed off line. A binning of the data in 1° and 2° intervals was chosen for the $Q$-value and cross-section measurements, respectively. The overall energy resolution achieved was about 30 keV and 40 keV for the measurements on $^{204}$Hg and $^{206}$Pb, respectively (see Fig. 1).

The beam was monitored using an internal Faraday cup within the scattering chamber for angle settings $\Theta_{K600} \leq 15°$ and, with a more accurate external Faraday cup, at larger angles. The $\Theta_{K600} = 15°$ setting served as the overlap angle. The beam polarization was measured using the well-known analyzing power of the $^3$He($\vec{d}$,$p$)$^4$He reaction as described in Ref. [17] and amounted to typically $P_y \approx 0.55$.

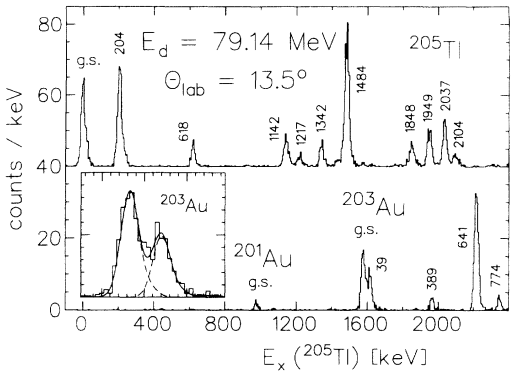


FIG. 1. Comparison of ($d$,$^3$He) spectra on $^{206}$Pb (top) and $^{204,202}$Hg (bottom) at $\Theta_{lab} = 13.5°$. The inset shows the result of a peak-fitting procedure for the ground state and first excited state of $^{203}$Au.

The accuracy of the reconstruction of scattering angles and the detector acceptance were checked by using a multiple-slit aperture at the spectrograph entrance which contained five narrow slits at precisely known scattering angles.

Target thicknesses were determined relative to that of a well-known $^{208}$Pb target by measuring elastic deuteron scattering at forward angles, employing small apertures, and a subsequent optical-model analysis of the cross sections. We used a self-supporting $^{206}$Pb target of thickness 0.55 mg/cm$^2$ and 94.9% isotopic enrichment. The $^{204}$Hg target was HgS of thickness 0.16 mg/cm$^2$ on a 26 $\mu$g/cm$^2$ carbon backing; the isotopic enrichment of the mercury was 92.6% $^{204}$Hg and 4.8% $^{202}$Hg; $^{34}$S was enriched to 99.5%. The $^{34}$S enrichment instead of $^{nat}$S was chosen because the $Q$ value for the ($d$,$^3$He) reaction is $-5.4$ MeV as compared to $-3.4$ MeV for $^{32}$S. This opened a 2 MeV window for the unobstructed investigation of $^{204}$Hg which has a $Q$ value of $-3.3$ MeV. The stability of the HgS target was checked periodically by comparison with a HgS reference target on which only a tiny beam load was applied. No target degradation with time was observed.[1]

## III. RESULTS

### A. $Q$ values of the $^{202,204}$Hg($d$,$^3$He) reactions

Based on the $^{202,204}$Hg$(t,\alpha)$ experiment [12] the $Q$ value of the $^{202,204}$Hg($d$,$^3$He) reactions are given [18] as $Q(204) = -3359(15)$ keV and $Q(202) = -2754(15)$ keV, respectively. As the $Q$ value of the $^{206}$Pb($d$,$^3$He) reaction is known as $Q(206) = -1758.9(1.6)$ keV, i.e., with a

[1]We wish to thank Dr. H.-J. Maier, University of München, for preparing the HgS targets.

considerably smaller error, we utilized our parallel measurements of $(d,^3\mathrm{He})$ spectra on $^{206}$Pb and Hg targets for $Q$-value determinations. Note that this was only a by-product of our experiment whose accuracy suffered, e.g., from the different target thicknesses. Ideally one should have used a mixed Hg/Pb target for a simultaneous measurement.

Figure 1 shows a comparison of $\Theta_{\mathrm{lab}} = 13.5°$ spectra on $^{206}$Pb and HgS. They represent one-quarter bin of data taken with the K600 spectrograph moved to $\Theta_{\mathrm{K600}} = 15°$. The spectra have been linearized in energy by a linear fit through peak positions (e.g., in Fig. 1, top) corresponding to adopted $^{205}$Tl states (denoted by an asterisk in Table I), and a $\chi^2$ per degree of freedom of 1.32 was obtained. Similarly successful fits were obtained for all 1° bins of the runs with $\Theta_{\mathrm{K600}} = 15°, 17°$, and 20°. Column 2 of Table I contains the excitation energies in $^{205}$Tl resulting from averaging all fit results. Typical deviations from the currently adopted excitation energies amount to 0 – 2 keV for the more strongly excited states.

$Q$-value differences based on these energy calibrations were corrected for the different energy losses in the two targets. The influence of the carbon backings was also taken into account. These corrections, depending on the angle, amounted to about 5.5 (2.7) keV. In addition a small kinematical correction of about −2 keV was necessary to account for the different target masses. With these corrections the $Q$-value differences displayed in Fig. 2 were obtained. The open symbols denote the results from the 1° bins with error bars that include statistical errors and uncertainties from the above corrections added in quadrature. The solid symbols represent the weighed averages for each run with the dashed lines representing the resulting average errors. The error bar attached to the solid symbols in addition include a 5 keV systematic error added in quadrature. This estimated systematic error accounts for apparent instabilities in the magnetic components of the beam lines or the spectrograph occurring between Hg and Pb runs.

The average of the three data points (solid symbols) yields

$$Q(206) - Q(204) = 1582.0(3.0)\ \mathrm{keV}\ , \tag{2}$$

$$Q(206) - Q(202) = 979.9(3.1)\ \mathrm{keV}\ . \tag{3}$$

TABLE I. Spectroscopic results from the $^{206}$Pb$(\vec{d},^3$He$)^{205}$Tl reaction at $E_d = 79.1$ MeV.

| $E_x$ | $J^\pi$ | $E_x$ | $nlj$ | $C^2S$ | $E_x$ | $C^2S$ |
|---|---|---|---|---|---|---|
| Adopted levels[a] | | $(\vec{d},^3$He) at 79.1 MeV[b] | | | $(\vec{d},^3$He) at 79.4 MeV[c] | |
| 0.000[d] | $1/2^+$ | 0.000 | $3s_{1/2}$ | 1.27 | 0.000 | 1.09 |
| 0.204[d] | $3/2^+$ | 0.204 | $2d_{3/2}$ | 1.96 | 0.202 | 1.61 |
| 0.619[d] | $5/2^+$ | 0.618 | $2d_{5/2}$ | 0.44 | 0.618 | 0.38 |
| 0.924 | $7/2^+$ | 0.925 | $1g_{7/2}$ | 0.08 | | |
| 1.141[d] | $3/2^+$ | 1.142 | $2d_{3/2}$ | 0.83 | 1.139 | 0.74 |
| 1.219 | $1/2^+$ | 1.217 | $3s_{1/2}$ | 0.20 | 1.217 | 0.18 |
| 1.340[d] | $3/2^+$ | 1.342 | $2d_{3/2}$ | 0.43 | 1.340 | 0.37 |
| 1.434 | $(1/2^+)$ | 1.434 | $3s_{1/2}$ | 0.08 | 1.435 | 0.06 |
| 1.484[d] | $11/2^-$ | 1.484 | $1h_{11/2}$ | 7.35 | 1.486 | 6.31 |
| 1.574 | $(3/2^+)$ | 1.580 | $2d_{(5/2)}$ | 0.11 | 1.579 | 0.10 |
| | | 1.644 | $2d_{(5/2)}$ | 0.02 | | |
| | | 1.765 | $2d_{(3/2)}$ | 0.05 | | |
| 1.866 | $(5/2^+)$ | 1.848 | $2d_{5/2}$ | 0.59 | 1.844 | 0.54 |
| 1.951[d] (3) | $(5/2^+)$ | 1.949 | $2d_{5/2}$ | 0.83 | 1.949 | 0.74 |
| | | 2.037 | $2d_{5/2}$ | 0.97 | 2.035 | 0.85 |
| | | 2.104 | $2d_{5/2}$ | 0.26 | 2.098 | 0.28 |
| 2.304 | $(1/2, 3/2^+)$ | 2.305 | $2d_{5/2}$ | 0.03 | | |
| | | 2.410 | $2d_{5/2}$ | 0.10 | 2.434 | 0.06 |
| | | 2.479 | $1h_{11/2}$ | 1.22 | 2.498 | 0.94 |
| 2.583 | | 2.583 | $1h_{11/2}$ | 1.70 | 2.607 | 1.37 |
| 2.750 | $(1/2, 3/2^+)$ | 2.740 | $2d_{5/2}$ | 0.11 | 2.756 | 0.09 |
| 2.881 | $(5/2, 7/2)$ | 2.869 | $(2d_{5/2})$ | 0.07 | | |
| | | 2.942 | $(2d_{5/2})$ | 0.08 | | |
| 2.996 | | 2.998 | $(2d_{5/2})$ | 0.06 | | |
| | | 3.117 | $(2d_{5/2})$ | 0.17 | | |
| 3.287 | | 3.279 | $(2d_{5/2})$ | 0.05 | | |
| 3.363 | | 3.370 | $(2d_{5/2})$ | 0.05 | | |
| 3.531 | $(15/2, 17/2^+)$ | 3.525 | $(2d_{5/2})$ | 0.03 | | |

[a]Reference [19].
[b]This work.
[c]Reference [9].
[d]Adopted for energy calibration; errors are less than 0.1 keV, unless otherwise given.

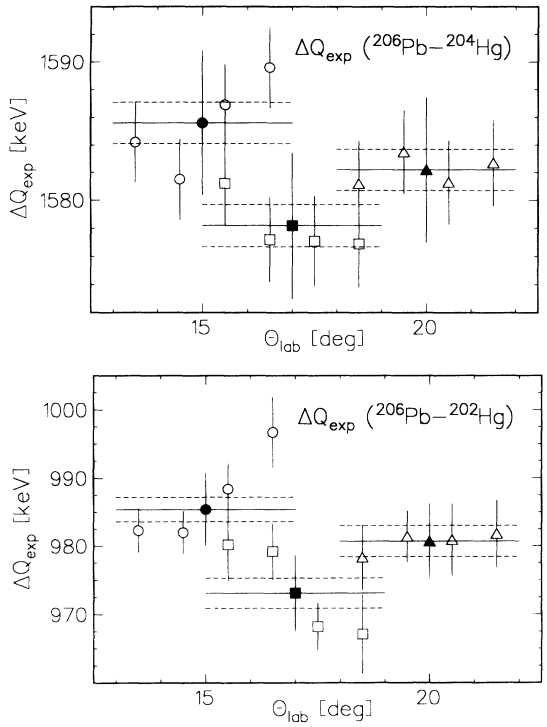


FIG. 2. $Q$-value differences for the target pairs $^{206}$Pb and $^{204}$Hg (top) and $^{206}$Pb and $^{202}$Hg (bottom), respectively, as measured at three central angles of the K600 spectrograph. Open symbols represent the data for 1° intervals. Solid symbols represent the average values of each run with the dashed lines indicating the average errors. The error bars of the average values include additional systematic errors (see text).

With the accepted $Q$ value for $^{206}$Pb [18] of $Q(206) = -1758.9(1.6)$ keV we obtain the final results

$$Q(204) = -3340.9(3.4) \text{ keV} \quad (4)$$

and

$$Q(202) = -2738.8(3.5) \text{ keV}. \quad (5)$$

These values agree with those from the $(t,\alpha)$ measurements [12] $Q(204) = -3359(15)$ and $Q(202) = -2754(15)$ just within the combined errors.

### B. Spectroscopic results

The spectroscopic information deduced from this experiment is based on the measured angular distributions and their DWBA analysis. Inspection of the data shows that the shapes of angular distributions of the differential cross sections and vector-analyzing powers are characteristic for the $l,j$ values of the transferred proton. Also they are remarkably stable over the energy and mass range covered. This allows for empirical $l$ and $j$ assignments by comparison to cases of known spin and parity (see, e.g., Fig. 4).

In a previous investigation of the $^{206}$Pb$(\vec{d},^3$He) reaction at 79.4 MeV [9] optical potentials and bound state potentials have been studied in great detail and very satisfactory DWBA descriptions of the measured data were obtained. Adopting the optical potentials D2 and H2 of Ref. [9], we performed exact finite-range DWBA calculations with the code DWUCK5 [20]. Standard nonlocality corrections of $\beta = 0.54$ and $\beta = 0.25$ were used in all DWBA calculations for the deuteron and $^3$He optical potentials, respectively. The bound-state parameters B1 were also taken from Ref. [9]; of the two prescriptions for bound-state potentials discussed there, we chose the conventional well-depth procedure. Except for trivial $Z,A$ adjustments, which were applied in the case of $^{202,204}$Hg targets, all DWBA fits and spectroscopic factors shown in the following are based on such DWBA calculations.

#### 1. $^{206}$Pb$(\vec{d},^3$He$)^{205}$Tl results

Figure 3 shows a typical spectrum of the $^{206}$Pb$(\vec{d},^3$He) reaction. The energy resolution of about 40 keV [full width at half maximum (FWHM)] is better than the 60 keV resolution obtained in the previous experiment [9] using the QDDM spectrograph at IUCF. Also the statistical accuracy is higher and the background somewhat lower. This may explain our observation of some weak transitions not located previously (see Table I).

Figure 4 contains angular distributions of the strongest transition for each relevant $l$ and $j$ transfer (see also Figs. 5–9). Except for the weakly excited $7/2^+$ at 925 keV the differential cross sections and vector-analyzing powers are very well described by the DWBA calculations. Note, in particular, the characteristically opposite phases of the vector-analyzing powers for $d_{3/2}$ and $d_{5/2}$ transitions, respectively. Based on such patterns we propose the $l,j$ assignments as given in column 4 of Table I. They agree in all cases with the assignments made in the previous $^{206}$Pb$(\vec{d},^3$He) experiment [9]. Two assignments ($E_x = 2305$ and 2740 keV) appear to disagree with the adopted assignments [19] for close-by levels; of course we cannot exclude that different states were populated. Some previously tentative assignments are now unambiguous ($E_x = 1434, 1848, 1949$ keV).

As Table I shows, our absolute spectroscopic factors are typically 10–15 % larger than those values from Ref. [9], which also been deduced using the well-depth

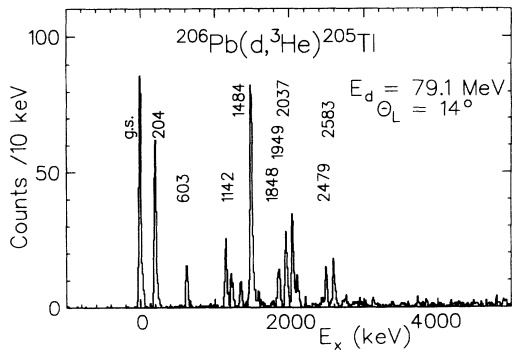


FIG. 3. Spectrum of the $^{206}$Pb$(d,^3$He) reaction at 79.1 MeV.

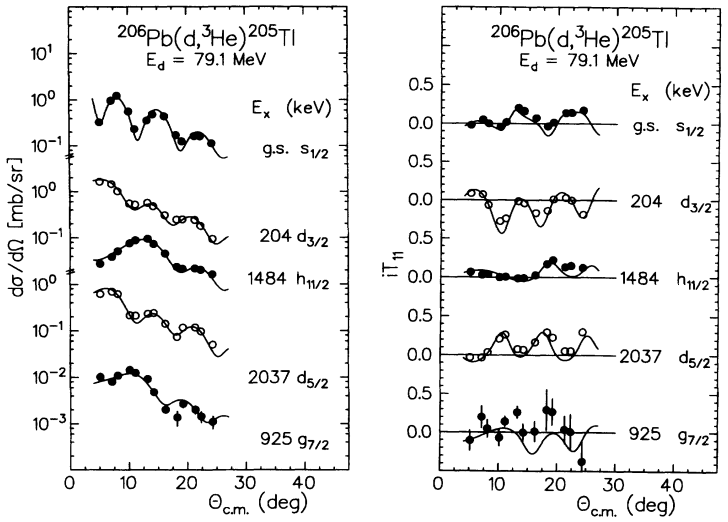


FIG. 4. Angular distributions of cross sections (left) and vector-analyzing powers (right) for the $^{206}$Pb($\vec{d}$,$^{3}$He)$^{205}$Tl reaction at 79.1 MeV. Solid curves represent the results of DWBA calculations assuming $l$ and $j$ transfers as indicated.

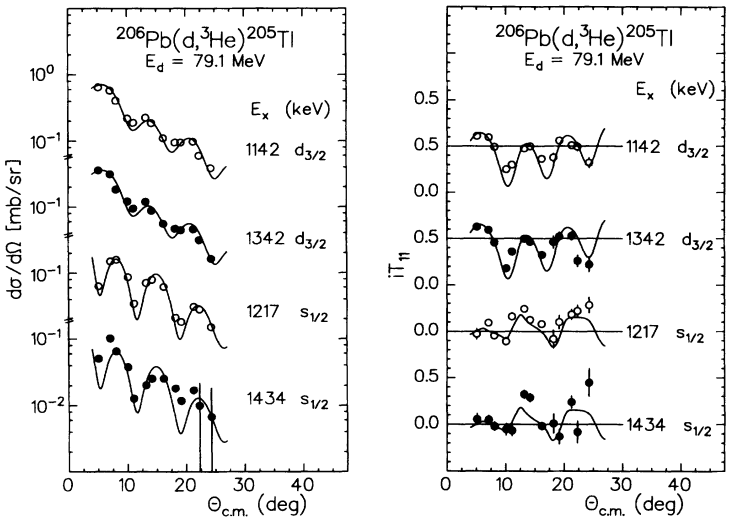


FIG. 5. Angular distributions of cross sections (left) and vector-analyzing powers (right) for the $^{206}$Pb($\vec{d}$,$^{3}$He)$^{205}$Tl reaction at 79.1 MeV. Solid curves represent the results of DWBA calculations assuming $l$ and $j$ transfers as indicated.

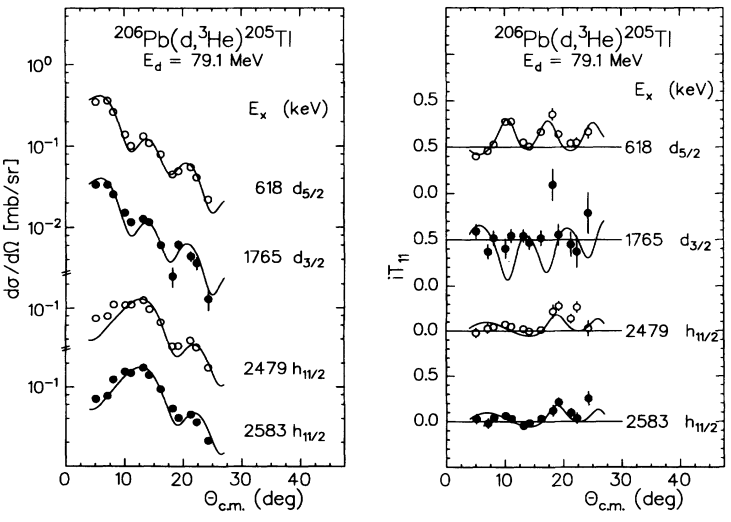


FIG. 6. Angular distributions of cross sections (left) and vector-analyzing powers (right) for the $^{206}$Pb($\vec{d}$,$^{3}$He)$^{205}$Tl reaction at 79.1 MeV. Solid curves represent the results of DWBA calculations assuming $l$ and $j$ transfers as indicated.

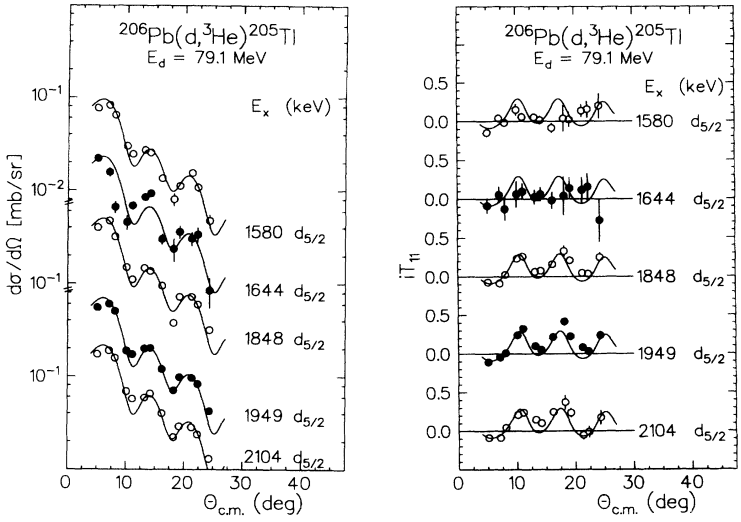


FIG. 7. Angular distributions of cross sections (left) and vector-analyzing powers (right) for the $^{206}$Pb($\vec{d}$,$^{3}$He)$^{205}$Tl reaction at 79.1 MeV. Solid curves represent the results of DWBA calculations assuming $l$ and $j$ transfers as indicated.

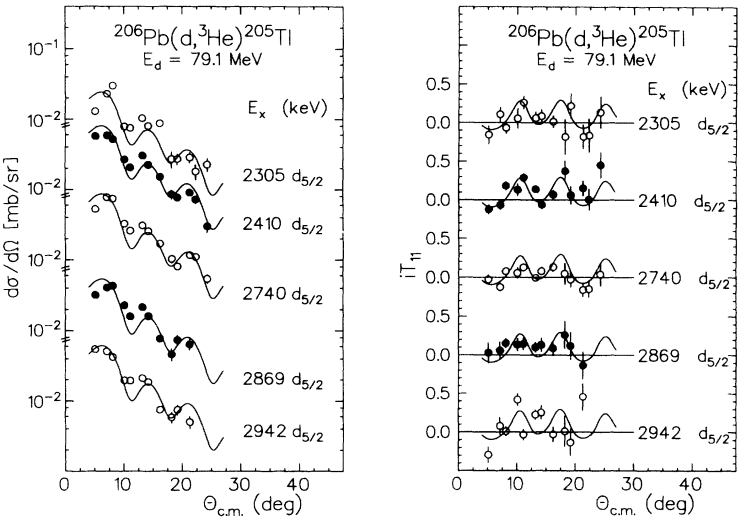


FIG. 8. Angular distributions of cross sections (left) and vector-analyzing powers (right) for the $^{206}$Pb($\vec{d}$,$^{3}$He)$^{205}$Tl reaction at 79.1 MeV. Solid curves represent the results of DWBA calculations assuming $l$ and $j$ transfers as indicated.

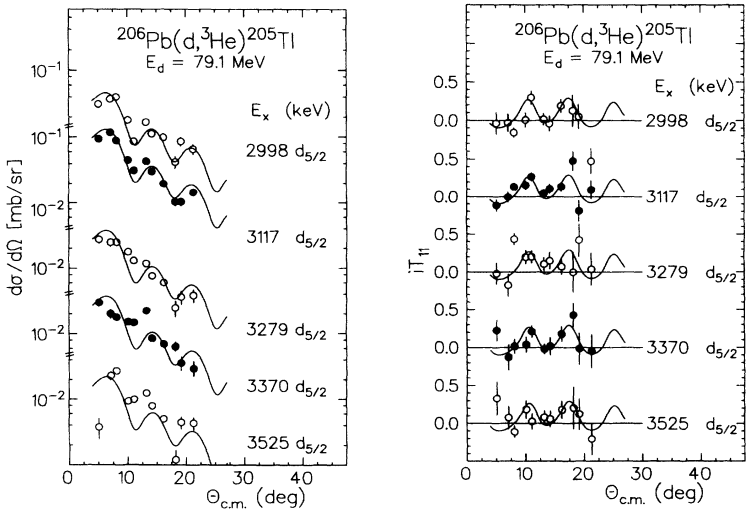


FIG. 9. Angular distributions of cross sections (left) and vector-analyzing powers (right) for the $^{206}$Pb($\vec{d}$,$^{3}$He)$^{205}$Tl reaction at 79.1 MeV. Solid curves represent the results of DWBA calculations assuming $l$ and $j$ transfers as indicated.

TABLE II. Spectroscopic results from the $^{204}$Hg($\vec{d}$,$^3$He)$^{203}$Au reaction at $E_d$ = 79.1 MeV.

| $E_x$ | $J^\pi$ | $E_x$ [MeV][d] | $nlj$ | $C^2S$ | $C^2S$ |
|---|---|---|---|---|---|
| Adopted[a,b] | | | $\vec{d}$,$^3$He)[c] | | $(t,\alpha)$ [b] |
| 0.000 | $3/2^+$ | 0.000 | $2d_{3/2}$ | 2.35 | 5.05 |
| 0.039 | $1/2^+$ | 0.039 | $3s_{1/2}$ | 0.64 | 1.52 |
| 0.386 | $3/2^+$ | 0.389 | $2d_{3/2}$ | 0.39 | 0.82 |
| 0.637 | $11/2^-$ | 0.641 | $1h_{11/2}$ | 7.87 | 7.30 |
| 0.760 | $5/2^+$ | 0.774 | $2d_{5/2}$ | 0.44 | 0.54 |
| 0.851 | | | | | |
| (0.985) | | 0.987 | $2d_{5/2}$ | 0.08 | |
| 1.087 | $5/2^+$ | 1.087 | $2d_{5/2}$ | 3.38 | 3.61 |
| 1.278 | $1/2^+$ | 1.284 | $3s_{1/2}$ | 0.12 | 0.20 |
| 1.460 | $11/2^-$ | 1.457 | $1h_{11/2}$ | 3.28 | 3.37 |
| | | 1.590 | $2d_{5/2}$ | 0.13 | |
| 1.759 | $(5/2^+)$ | 1.755 | $2d_{5/2}$ | 0.54 | (0.65) |
| | | 1.839 | $2d_{5/2}$ | 0.07 | |

[a]Reference [13].
[b]Reference [12].
[c]This work.
[d]Estimated error 3 keV.

procedure. With the DWBA calculations being identical the origin of this discrepancy rests in the slightly higher differential cross sections from the present experiment, which might result from uncertain wire efficiencies.

### 2. $^{204}$Hg($\vec{d}$,$^3$He)$^{203}$Au results

Figure 10 shows a typical spectrum of the $^{204}$Hg($\vec{d}$,$^3$He) reaction (see also Figs. 11 and 12 ). No significant strength could be located beyond $E_x$ = 1900 keV. This agrees with the findings of the $(\vec{t},\alpha)$ experiment [12]. The spectroscopic results are presented in Table II. We confirm all spin assignments, including the previously tentative $5/2^+$ assignment of the 1755 keV state. Two previously unknown $5/2^+$ states at 1590 and 1839 keV have been located. The probable doublet at 851 keV [12, 13][2] was not seen by us. The existence of a 987 keV level, previously uncertain, is confirmed. The estimated error of all excitation energies is 3 keV.

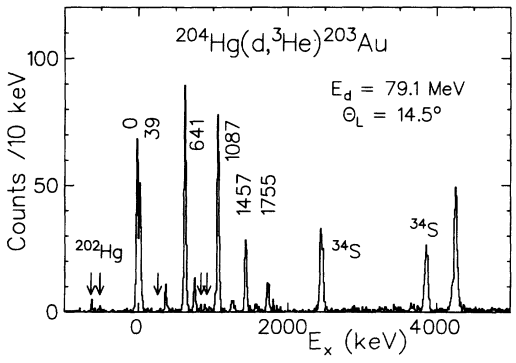


FIG. 10. Spectrum of the $^{204}$Hg($d$,$^3$He)$^{203}$Au reaction. Arrows indicate groups attributed to $^{202}$Hg admixtures in the target.

Our main interest naturally is devoted to the spectroscopic factors, notably of $1/2^+$ states in $^{203}$Au, which are needed for the CERES application. There substantial discrepancies, exceeding occasionally a factor of 2, are observed. Given the comparatively low quality of the fits of Ref. [12] and the typical problems of the $(\vec{t},\alpha)$ reaction in that mass region [21], we shall disregard the $(t,\alpha)$ spectroscopic factors in the following discussion. Note, e.g., that the summed $2d_{3/2}$ strength exceeds the shell-model limit of 4 by 50% when using the $(t,\alpha)$ spectroscopic factors. Interestingly, for high-spin transitions, such as $h_{11/2}$, where the angular momentum mismatch of the $(t,\alpha)$ reaction is reduced, the DWBA fits of the $(t,\alpha)$ cross sections are indeed fair and the $(t,\alpha)$ spectroscopic factors agree with those from the present experiment to better than 10%.

### 3. $^{202}$Hg($\vec{d}$,$^3$He)$^{201}$Au results

For the strongest transitions of the $^{202}$Hg($\vec{d}$,$^3$He) reaction angular distributions could be obtained even though the $^{202}$Hg enrichment was only about 4.8%. For excitation energies above 600 keV the association with $^{201}$Au states rests on previous identifications with separated isotopes [12]. For the sake of documentation we give our results in Fig. 13 and Table III. All previous spin and parity assignments are confirmed, with our assignment being somewhat uncertain for the 1459 keV state. The spectroscopic factors from the present experiment are again deemed more reliable than those from the $(t,\alpha)$ experiment for the reasons given above.

[2]This is erroneously quoted as 931 keV in Ref. [13].

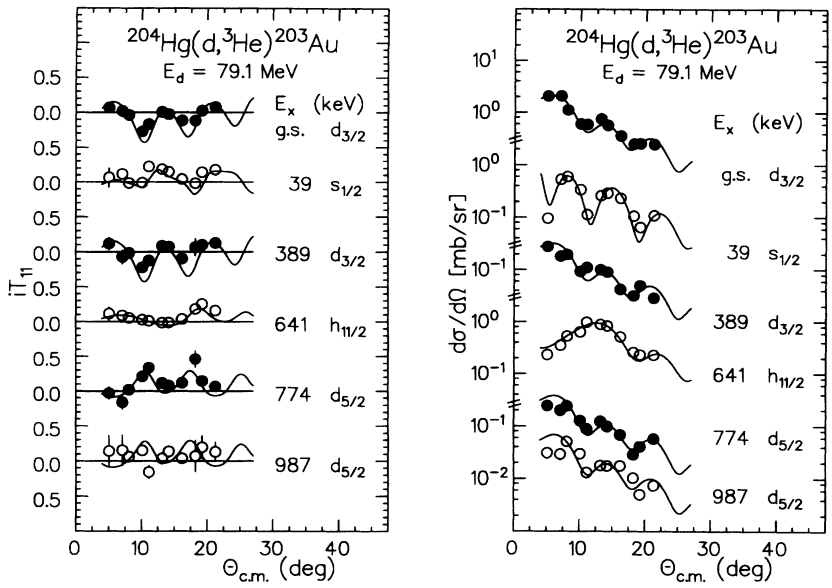


FIG. 11. Angular distributions of cross sections (left) and vector-analyzing powers (right) for the $^{204}$Hg($\vec{d}$,$^3$He)$^{203}$Au reaction at 79.1 MeV. Solid curves represent the results of DWBA calculations assuming $l$ and $j$ transfers as indicated.

## IV. DISCUSSION OF 3*s*-PROTON OCCUPANCIES

### A. Occupancies in $^{206}$Pb and $^{204}$Hg

With the present data the 3*s*-proton occupancy in the ground state of $^{206}$Pb may be deduced in two ways. The most direct and conventional way is to apply the sum rule of French and Macfarlane [1], which in the present case reads

$$\Sigma' S(206) \leq \Sigma S(206) = n(206), \tag{6}$$

where $\Sigma'$ again represents the sum of $3s_{1/2}$ spectroscopic factors taken over the observable part of the hole state spectrum. Clearly this truncated sum will not include high-lying strength in $^{205}$Tl as might result from tensor and short-range correlations. Hence the sum-rule value represents only a lower limit of the occupancy.

This sum rule was used [9] with spectroscopic factors derived from the earlier $^{206}$Pb($\vec{d}$,$^3$He) experiment to obtain $n(206) \geq 1.33$. With the $3s_{1/2}$ cross sections and spectroscopic factors from the present experiment being $\approx 15\%$ larger, application of Eq. (6) would lead to $n(206) \geq 1.55$.

The 15% difference in cross sections between the two ($\vec{d}$,$^3$He) experiments is certainly within the error that one would normally quote for absolute cross sections. Nevertheless the derived occupation probabilities of $\geq 66\%$ and $\geq 78\%$, respectively, convey a qualitatively different many-body picture of $^{206}$Pb. This experience should serve as another warning against the use of the conven-

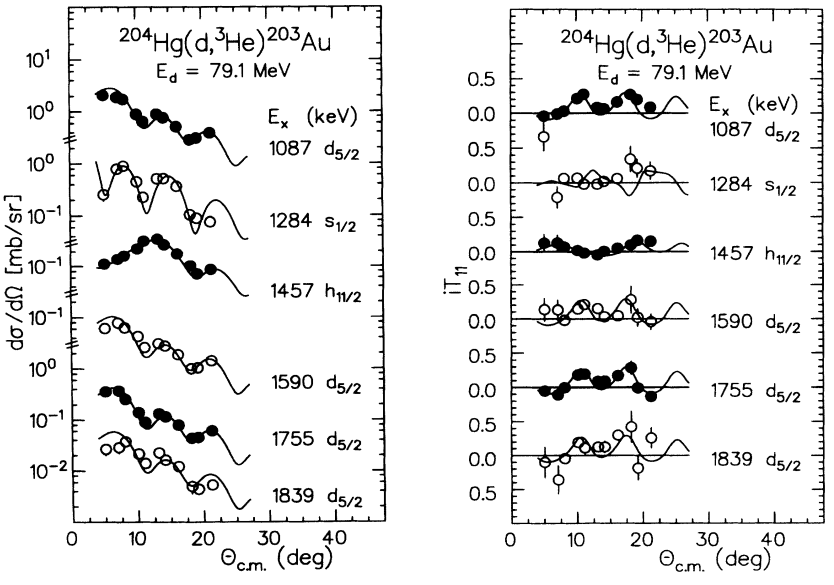


FIG. 12. Angular distributions of cross sections (left) and vector-analyzing powers (right) for the $^{204}$Hg($\vec{d}$,$^3$He)$^{203}$Au reaction at 79.1 MeV. Solid curves represent the results of DWBA calculations assuming $l$ and $j$ transfers as indicated.

TABLE III. Spectroscopic results from the $^{202}$Hg($\vec{d}$,$^3$He)$^{201}$Au reaction at $E_d$ = 79.1 MeV.

| $E_x$ | $J^\pi$ | $E_x$ [MeV][c] | $nlj$ | $C^2S$ | $C^2S$ |
|---|---|---|---|---|---|
| Adopted[a] | | | ($\vec{d}$,$^3$He) [b] | | ($t,\alpha$) [d] |
| 0.000 | $3/2^+$ | 0.000 | $2d_{3/2}$ | 2.90 | 3.81 |
| 0.101 | $1/2^+$ | 0.094 | $3s_{1/2}$ | 0.60 | 0.93 |
| 0.897 | $1/2^+$ | 0.907 | $3s_{1/2}$ | 0.27 | 0.35 |
| 1.465 | $5/2^+$ | 1.459 | $2d_{5/2}$ | 2.04 | 1.02 |
| 1.506 | $11/2^-$ | 1.508 | $1h_{11/2}$ | 3.66 | 3.10 |

[a]Reference [22].
[b]This work.
[c]Errors in excitation energies are estimated as 5 keV.
[d]Reference [12].

tional sum rule given by Eq. (6) without appropriate caution. It also justifies *a posteriori* our rationale in remeasuring the ($\vec{d}$,$^3$He) reaction on $^{206}$Pb in parallel with that on $^{204}$Hg with the purpose of obtaining precise *relative* spectroscopic factors.

The second approach to the 3*s*-proton occupancies is provided by the CERES method, Eq. (1). As mentioned in the Introduction, this method uses relative spectroscopic factors and accounts approximately for the cut off of high-energy tails in the hole strength function. With the spectroscopic strengths from Tables I and II and the value $z' = 1.02(10)$ from Ref. [10], we obtain $n(206) \simeq 1.96(23)$. The large error, which even encompasses unphysical values $n(206) > 2$, shows the influence of the uncertainties of input quantities on the CERES result; the biggest uncertainty stems from the model dependence of $z'$. Nevertheless, the result is consistent with that derived from the direct application of the French-Macfarlane sum rule and may be taken as yet another indication of a relatively high 3*s* occupancy in $^{206}$Pb.

To avoid the uncertainties in the value of $z'$ it has been suggested [3] that one should use Eq. (1) for a prediction of $z'$. To that aim the value of $n(206) = 1.35(14)$ will be adopted from the previous CERES application [3]. This value rests on the $^{206}$Pb–$^{205}$Tl charge difference which we consider more reliable because the charge densities of $^{205}$Tl and $^{206}$Pb were measured in parallel [4] while the $^{204}$Hg($e,e$) experiment [10] was performed independently. With the spectroscopic factors from the present experiment, Eq. (1) yields $z' = 0.75(18)$.

This prediction of $z'$ is more than one standard deviation lower than the average value of $z' = 1.02(10)$ taken from Ref. [10]. But it is compatible with the value $z' = 0.94(5)$ resulting from the use of the $G_\sigma$ force alone in the Hartree-Fock calculations of Ref. [10].

Following the traditional use of absolute spectroscopic factors one may test our result for $z'$ by simply calculating

$$z' \simeq \Sigma' S(206) - \Sigma S'(204) \quad . \tag{7}$$

In fact, in this application of the French-Macfarlane sum rule the uncertainty resulting from the truncation

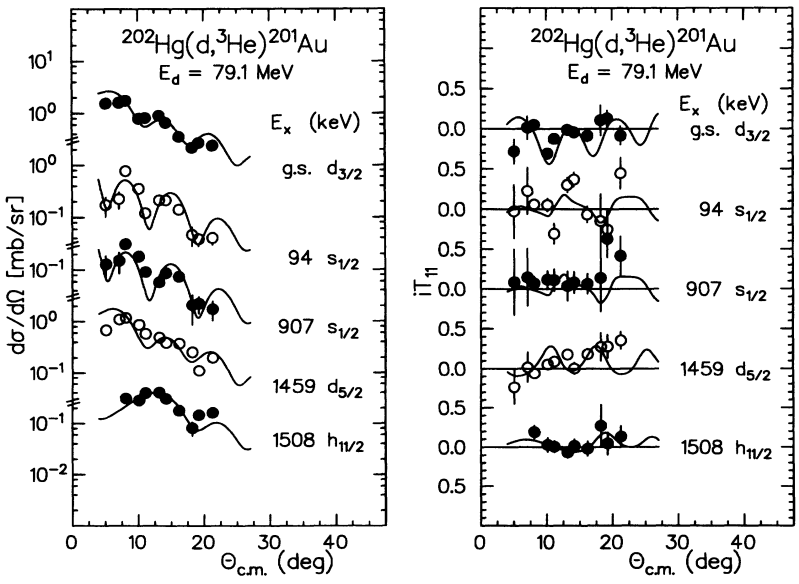


FIG. 13. Angular distributions of cross sections (left) and vector-analyzing powers (right) for the $^{202}$Hg($\vec{d}$,$^3$He)$^{201}$Au reaction at 79.1 MeV. Solid curves represent the results of DWBA calculations assuming $l$ and $j$ values of the transferred proton as indicated.

of the spectroscopic sums is likely to cancel partially. What remains, however, is the uncertainty of absolute spectroscopic factors which is avoided by the CERES method. With the spectroscopic factors from Tables I and II we have $\Sigma' S(206) = 1.55$ and $\Sigma' S(204) = 0.76$; hence $z' \simeq 0.79$. This compares very well with the result $z' = 0.75(18)$ based on the sum rule Eq. (1) and on a value of $n(206)$ which was determined previously [3] using an entirely independent input. The internal consistency of these different methods is very satisfying.

With the value of $z' = 0.75(18)$ at hand we may finally obtain an estimate of the $3s$-proton occupancy $n(204)$ in the ground state of $^{204}$Hg that is independent of any *absolute* spectroscopic factors. To that aim we recall the definition of $z' = n(206) - n(204)$ and, again, adopt the value $n(206) = 1.35(14)$ from Ref. [3]. The resulting value for $^{204}$Hg, $n(204) = 0.60(23)$, unfortunately is subject to a large error. However it does indicate a substantial $3s$-proton occupancy in the ground state of $^{204}$Hg, as does the direct use of the French-Macfarlane sum rule [analogous to Eq. (6)] with the spectroscopic strength from Table II which leads to $n(204) \geq 0.76$.

### B. Summary of 3s-proton occupancies in the lead region

A review of the $3s$-proton occupancies in the Pb region as derived by CERES from a network of $(e, e'p)$ and $(d,^3\mathrm{He})$ experiments has recently been given [3]. In the light of the present experiments we present an update of that summary. We chose to select the following data for this summary. (i) The $3s$-proton part of the $^{206}$Pb – $^{205}$Tl charge difference has been evaluated as $z = 0.7(1)$ originally [5] and as $z = 0.64(6)$ more recently [23]. We retain only the more recent value in the following. (ii) As discussed above, we consider the result of $z'$ from Ref. [10] as strongly affected by model uncertainties. Instead we adopt $z' = 0.75(18)$ and the subsequent value of $n(204)$, as derived above using the pickup strengths from the present work and $n(206)$ from Ref. [3]. The resulting $3s$-proton occupancies are summarized in Table IV.

Finally, in Fig. 14, a comparison of these results is made with simple shell-model predictions. Noteworthy of course, is the 20–30% depletion of the $3s$-proton shell for the doubly magic nucleus $^{208}$Pb. The value for $n(208)$ appears perfectly compatible with the—necessarily truncated—sum of absolute spectroscopic factors from $(e, e'p)$ experiments [24], $\Sigma' S(208) = 0.65(5)$, if one keeps in mind that $n(208) \geq \Sigma' S(208)$ as discussed above. The explanation of this depletion is a subject of considerable interest for many-body theories (see Ref. [3] and references given there). As the present data do not contribute to the $^{208}$Pb problem we shall not dwell on this question here. Suffice it to recall that a depletion of about 10% is typically attributed to the long-range correlations of random phase approximation (RPA) type, and an amount varying between 10% and 30% is expected to result from short-range correlations.

TABLE IV. $3s$-proton occupancies.

| Nucleus | $n$ |
|---|---|
| $^{208}$Pb | 1.54(17)[a] |
| $^{206}$Pb | 1.35(14)[a] |
| $^{205}$Tl | 0.71(16)[a] |
| $^{204}$Hg | 0.60(23)[b] |

[a]Reference [3].
[b]Present work.

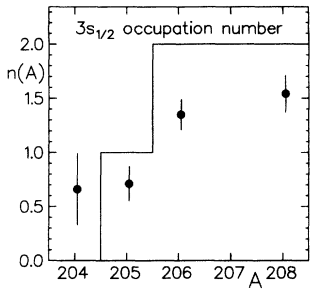


FIG. 14. Summary of $3s$-proton occupation numbers $n(A)$ for $^{204}$Hg, $^{205}$Tl, $^{206}$Pb, and $^{208}$Pb, as derived with the CERES method. Simple shell-model values (histogram) are shown for comparison.

In contrast, much of the deviations from the simple shell-model predictions that Fig. 14 shows for nuclei lighter than $^{208}$Pb is qualitatively attributed to long-range effects, such as configuration mixing and deformations. The role of configuration mixing for the spectroscopic results on $^{206}$Pb has been discussed earlier [15] in terms of a phonon-hole coupling model [25]. For proton pickup in $^{204}$Hg a qualitative discussion in the same framework has been given by Flynn *et al.* [12] who point out the role of the increased collectivity of the $^{204}$Hg core over $^{206}$Pb. This is recognized from the energies [$B(E2)$ values] of the first $2^+$ states which are 0.80 MeV [6.8 Weisskopf unit (W.u.)] and 0.44 MeV (15.4 W.u.) for $^{206}$Pb and $^{204}$Hg, respectively. In the absence of detailed shell-model calculations we have to leave the discussion at this qualitative level.

## V. CONCLUSIONS

The parallel investigations of the $(\vec{d},^3\mathrm{He})$ reactions on $^{204}$Hg and $^{206}$Pb at 79.1 MeV have produced considerable spectroscopic information. In particular we obtained an improved mass determination for $^{203}$Au and—as a byproduct—$^{201}$Au; both results agree with the previous values within the combined errors. Spin and parity assignments based on previous $^{206}$Pb$(\vec{d},^3\mathrm{He})$ and $^{204}$Hg$(\vec{t},\alpha)$ experiments were confirmed. The cross sections and absolute spectroscopic factors from the present measurement on $^{206}$Pb are about 15% larger than those from a previous experiment. The spectroscopic factors for the pickup reaction on $^{204}$Hg differ strongly from those of the $(\vec{t},\alpha)$ experiment. Judged by the quality of the fits and the general systematics, the $(d,^3\mathrm{He})$ results seem superior to the $(t,\alpha)$ results. Therefore, we believe

that the present data represent the first reliable set of spectroscopic factors for proton removal from $^{204}$Hg.

The real motivation of the experiment and the focus of the discussion was the application of the CERES sum rule to the $^{204}$Hg-$^{206}$Pb pair of nuclei. For that purpose accurate *relative* spectroscopic sums for $3s_{1/2}$-proton removal were required. The CERES method was applied in two ways. The straightforward application based on the charge densities of $^{204}$Hg and $^{206}$Pb suffered from the substantial uncertainties entering into a mean-field interpretation of the charge density differences. In the second method we adopted the 3*s*-proton occupancy in the ground state of $^{206}$Pb from an independent source and deduced the corresponding number for $^{204}$Hg. We emphasize that this evaluation utilized only *relative* spectroscopic factors. Therefore it was interesting to observe that the difference of the 3*s*-proton occupancies for $^{206}$Pb and $^{204}$Hg agrees with that obtained by applying the conventional French-Macfarlane sum rule directly with our *absolute* spectroscopic factors.

Finally we presented an overview of 3*s*-proton occupancies as an overall result of the CERES experiments performed to date. We observed that this set of occupancies possesses internal consistency and stands several cross checks. The findings may be summarized by stating that the 3*s*-proton occupancy increases from about 0.6 protons to about 1.5 protons in going from $^{204}$Hg to $^{208}$Pb. According to our present understanding both short-range and long-range correlations in nuclei are essential for reproducing these occupancies.

This work was supported in part by the German Federal Minister for Research and Technology (BMFT) under Contract Number 06 TÜ 243, and in part by the U.S. National Science Foundation under Grant NSF PHY 87-14406.

[1] J.B. French and M.H. Macfarlane, Nucl. Phys. **26**, 168 (1966).
[2] G.J. Wagner, in *Nuclear Structures at High Spin, Excitation and Momentum Transfer (McCormick's Creek State Park, Bloomington, Indiana)*, Proceedings of the Workshop on Nuclear Structure at High Spin, Excitation and Momentum Transfer, edited by Herman Nann, AIP Conf. Proc. No. 142 (AIP, New York, 1985), p. 220.
[3] P. Grabmayr, Prog. Part. Nucl. Phys. **29**, 221 (1992) and references therein.
[4] J.M. Cavedon *et al.*, Phys. Rev. Lett. **49**, 978 (1982).
[5] B. Frois *et al.*, Nucl. Phys. **A396**, 409c (1983).
[6] P.K.A. de Witt Huberts, J. Phys. G. **16**, 507 (1990).
[7] D.S. Onley, in Proceedings of the 8th Seminar on Electromagnetic Interactions at Low and Medium Energies, edited by R.A. Eramzhian, Report No. AH CCCP, 1991 (unpublished), p. 116.
[8] J.M. Udias, P. Sarriguren, E. Moya de Guerra, and J.A. Caballero, Phys. Rev. C (to be published).
[9] M.C. Radhakrishna *et al.*, Phys. Rev. C **37**, 66 (1988).
[10] A.J.C. Burghardt, Ph.D. thesis, University of Amsterdam (1988).
[11] F. Tondeur, Phys. Lett. **123B**, 139 (1983).
[12] E.R. Flynn *et al.*, Phys. Lett. **105B**, 125 (1981).
[13] M.R. Schmorak, Nucl. Data Sheets **46**, 287 (1985).
[14] P. Grabmayr *et al.*, J. Phys. G **18**, 1753 (1992).
[15] P. Grabmayr *et al.*, Phys. Lett. **164B**, 15 (1985).
[16] E.N.M. Quint *et al.*, Phys. Rev. Lett. **58**, 1088 (1987).
[17] E.J. Stephenson *et al.*, Phys. Rev. C **28**, 134 (1983).
[18] A.H. Wapstra and G. Audi, Nucl. Phys. **A432**, 55 (1985).
[19] M.R. Schmorak, Nucl. Data Sheets **45**, 145 (1985).
[20] P.D. Kunz, computer code DWUCK5.
[21] E.R. Flynn, R.A. Hardekopf, J.D. Sherman, J.W. Sunier, and J.P. Coffin, Nucl. Phys. **A279**, 394 (1977).
[22] M.E. Schmorak, Nucl. Data Sheets **49**, 733 (1986).
[23] I. Sick and P.K.A. de Witt Huberts, Commun. Nucl. Part. Phys. **40**, 177 (1991).
[24] L. Lapikas, Nucl. Phys. **A553**, 297c (1993).
[25] L. Zamick, V. Klemt, and J. Speth, Nucl. Phys. **A245**, 365 (1975).